

HEAD AND NECK CANCER PATIENT SIMILARITY BASE ON ANATOMICAL STRUCTURAL GEOMETRY

Chia-Chi Teng¹, Linda G. Shapiro^{1,2}, Ira Kalet^{2,3}

¹Department of Electrical Engineering, ²Department of Computer Science
³Department of Radiation Oncology, University of Washington

ABSTRACT

As we develop radiation treatment planning systems for head and neck cancer patients, there is a need to identify reference patients whose anatomical structures share similar features. By finding previously treated patients or prototypical models with the most similar anatomy in the head and neck region, our prototype system can do a better job of identifying lymph node regions based on known regions predefined for similar patients. This can potentially expedite the radiation treatment planning process which currently depends on oncologists manually delineating lymph node regions for each patient slice by slice on their CT scans. Our methodology uses the identification of landmark anatomical structures from the CT scan of the cancer patient and the computation of a Hausdorff distance between these and the corresponding structures of the reference scans. The combination of these structural correspondence features and a set of global shape features provide a distance metric that can rapidly find the most similar reference patient case and thus efficiently and accurately generate the desired lymph node regions for a given test case.

1. INTRODUCTION

With the recent advancement of modeling, scanning and visualizing techniques for 3D shapes, the amount and availability of digital 3D models have been drastically expanded. The subject of matching 3D shapes for content-based 3D shape retrieval has been of interest to many researchers in computer vision and computer graphics. Research groups of Princeton University [1] and National Taiwan University [2], and Utrecht University [3] have experimental systems that search similar 3D models of a given target object.

These traditional 3D shape retrieval systems mostly experiment with artificial models such as CAD models, 3D laser scanner output, or partial 3D shape surfaces in VRML. They also mostly focus on classifying 3D models of very different shapes, for example, airplane versus car, or human

versus dog. While these experimental systems can match models of the same classes to a certain degree of success, they usually fall short of distinguishing the finer details of objects within a class.

As we develop a radiation treatment planning system for head and neck cancer patients [7][8], there is an increasing need to identify similar patients whose anatomical structures share similar properties or features. By finding previously treated patients or canonical models with the most similar anatomy in the head and neck region, our system can generate possible lymph node regions for a target patient based on known regions defined in similar patients. We can in turn expedite the radiation treatment planning process, which currently depends on oncologists manually delineating lymph node regions for each patient slice by slice on their CT scans.

Using 3D medical images to find similarity among a known set of patients is becoming a research subject of interests in many medical domains. Ruiz *et al.* [9] use a shape-based similarity measure to find similar craniosynostosis patients for intervention planning. We are proposing a method to find similar head and neck cancer patients for radiation planning. The similarity of head and neck anatomy between patients is based not only on shape features of structures, such as outer body volume, mandible, and hyoid, but also on the relative location. These types of medical-image-based problems are very domain specific, and are not solved by the traditional shape-based retrieval system. This paper proposes a fast and effective way to find similar head and neck patients for the purpose of radiation treatment planning.

2. BACKGROUND RESEARCH

Recent reviews of 3D shape matching techniques was done by Iyer [4] and Tangelder [5]. A majority of the 3D shape matching systems use feature-based methods, which compare geometric and topological properties of 3D shapes. Methods using features or distributions work reasonably well in classifying objects of different shapes, but they are not discriminative about object details such as head and neck anatomy of different patients. The matching process is usually done by computing a distance between feature

vectors of different objects. Most systems do not give many details on the distance measurements or their comparison methods, although they usually imply a Euclidian vector space model and use either a simple (weighted) Euclidean distance or a city-block (L_1 Minkowski) distance.

As we need to compare similarity between anatomical structures from different patients, we do so by measuring the errors between structure surfaces using the 3D Hausdorff distance [10]. Given two aligned surface meshes, S_R and S_T , the distance between a point p_R belonging to S_R and the mesh S_T can be defined as follows:

$$d(p_R, S_T) = \min_{p \in S_T} \|p_R - p\|. \quad (1)$$

We first align meshes S_R and S_T with the Iterative Closest Point (ICP) rigid body registration [11]. Given the 3D point sets $P_R = \{p_i\}$ containing the n vertices of S_R , the registration process will produce a transformation matrix \mathbf{T} which minimize the function

$$D(S_R, S_T) = \sum_{i=1}^n d(Tp_i, S_T). \quad (2)$$

The transformed reference mesh TS_R consists of vertices $\{Tp_i\}$, and the Hausdorff distance between TS_R and S_T is given by

$$d_h(TS_R, S_T) = \max_{p \in S_R} d(Tp, S_T). \quad (3)$$

Image registration is commonly used in medical imaging applications. It is essentially a process of finding a geometric transformation \mathbf{g} between two sets of images, which maps a point \mathbf{x} in one image-based coordinate system to $\mathbf{g}(\mathbf{x})$ in the other. By assuming the head and neck anatomy has similar characteristics between a target patient and a reference person, we use image registration methods to transform a region from the reference image set to the target patient image set [7]. Mattes and Haynor [6] implemented a multi-resolution non-rigid (deformable) image registration method using B-splines and mutual information. The transformation of a point $\mathbf{x} = [x, y, z]^T$ in the reference image coordinate system to the target image coordinate system is defined by a 3×3 homogeneous rotation matrix \mathbf{R} , a 3-element transformation vector \mathbf{T} and a deformation term $\mathbf{D}(\mathbf{x}|\boldsymbol{\delta})$,

$$\mathbf{g}(\mathbf{x}|\boldsymbol{\mu}) = \mathbf{R}(\mathbf{x} - \mathbf{x}_C) - \mathbf{T}(\mathbf{x} - \mathbf{x}_C) + \mathbf{D}(\mathbf{x}|\boldsymbol{\delta}) \quad (4)$$

where \mathbf{x}_C is the center of the reference volume. A rigid body transformation defined by \mathbf{R} and \mathbf{T} is first calculated and used as the initial transformation for the deformation process. The deformation term $\mathbf{D}(\mathbf{x}|\boldsymbol{\delta})$ gives an x -, y -, and z -offset for each given \mathbf{x} . Hence the transformation parameter vector $\boldsymbol{\mu}$ becomes

$$\boldsymbol{\mu} = \{\gamma, \theta, \phi, t_x, t_y, t_z, \boldsymbol{\delta}_j\} \quad (5)$$

The first three parameters γ, θ, ϕ are the roll-pitch-yaw Euler angles of \mathbf{R} . The translation vector \mathbf{T} is defined by $[t_x, t_y, t_z]^T$. \mathbf{T} and \mathbf{R} together define the rigid body transformation. The parameter $\boldsymbol{\delta}_j$ is the set of the deformation coefficients. We incorporate similar image

registration techniques to align reference and target patients' CT images, and apply the resulting transformation \mathbf{g} to the known lymph node region contours to project the corresponding lymph node regions on the target patient CT images.

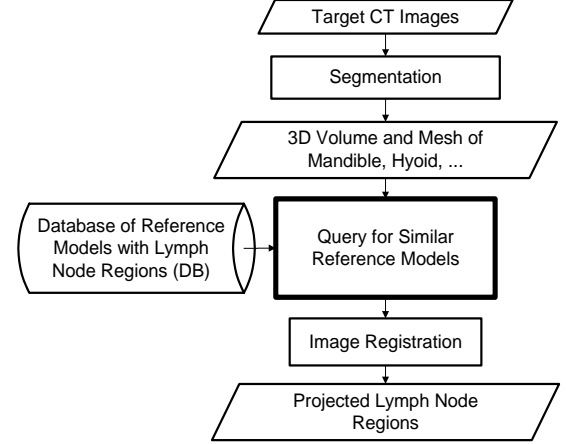


Fig. 1: Overall system block diagram.

3. SYSTEM OVERVIEW

We are given a stored database DB of CT scans from prototypical reference patients on which experts have drawn contours that denote the regions of interest. Given a single query CT scan Q from a target patient, we need to have a fast and effective way to determine the similarity between Q and each database image d in DB in order to find the most similar database images $\{d_s\}$. We will use the images from the query result as reference models for the 3D deformable image registration procedure [7] which is much more computationally complex and time consuming. Figure 1 is a simple block diagram that shows how the query process relates to the other component in the system.

The automatic segmentation process [8] selects a subset of axial slices, which is most relevant to the anatomy around the cervical lymph node regions, from the base of the skull to the thoracic inlet from each image set. Voxel volumes of anatomical structures of interest within that selected range of CT slices, including the mandible, hyoid bone, jugular veins, and outer body contour, are also produced from the segmentation process. 3D triangular surface meshes are generated for each segmented volume using the Visualization Toolkit (VTK, www.vtk.org), selected samples are shown in Figure 2.

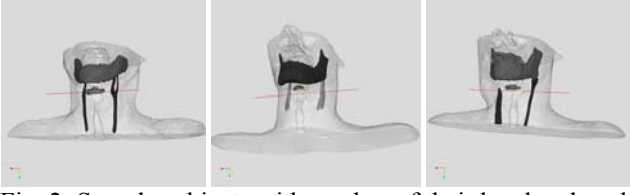


Fig. 2: Sample subjects with meshes of their head and neck volume between cranial base and thoracic inlet, mandible, hyoid, and jugular veins.

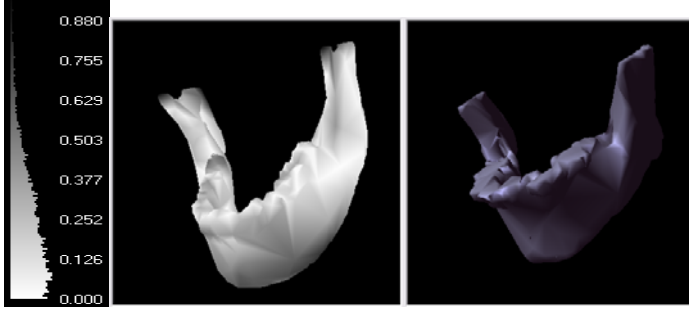


Fig. 3: Measuring Hausdorff distance (in centimeter) between mandible surface meshes from two patients.

4. FEATURE EXTRACTION

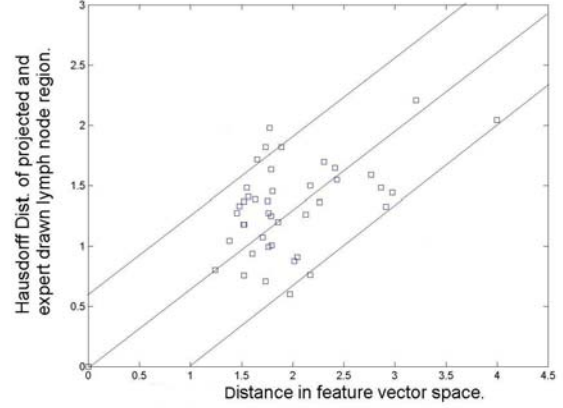
Image-based classification of head and neck lymph node regions has been proposed [12] to provide a more consistently reproducible nodal staging model for cancer patients. We use easily identifiable structures, including the mandible, hyoid, jugular veins and the outer body contour, that are relevant to the boundary for the lymph node regions to rapidly produce a distance metric between Q and each d in DB . The feature vectors that we use to compare two CT scans include three kinds of features: 1) simple numeric 3D regional properties of these structures, such as volume and extents, 2) vector properties or the relative location between structures and 3) shape properties or the surface meshes of these structures. Given feature vectors F_d and F_Q for models d and Q in the feature vector space \mathbb{R}^N , the following weighed Euclidean distance is used as the distance measure:

$$D(F_d, F_Q) = \left[\sum_{i=1}^N w_i d_i(F_{d_i}, F_{Q_i})^2 \right]^{\frac{1}{2}} \quad (6)$$

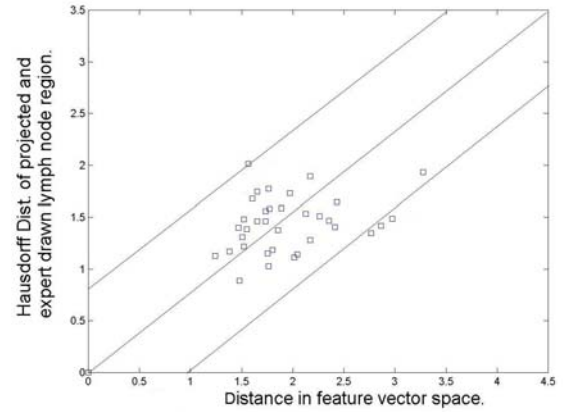
where w_i is the weight parameter, and d_i is the distance function for feature i ,

$$d_i(f_1, f_2) = \begin{cases} d_h(Tf_1, f_2) & \text{for mesh features} \\ |f_1 - f_2| & \text{otherwise} \end{cases} \quad (7)$$

and d_h is the Hausdorff distance defined in Equation 3, and T is the ICP registration transformation matrix.



(A)



(B)

Fig. 4: Comparison of distance measure in the feature vector space to the result of 3D deformable image registration, where the Y-axis represent the Hausdorff distance of the projected lymph node regions based on the registration transformation g to the expert hand drawn regions: (A) lymph node region 1B right, (B) 2B right.

The distance between mandible meshes of two subjects is one major discriminating feature of the proposed distance measure. Figure 2 shows the Hausdorff distance between the mandible surface meshes from two patients. The mesh on the left with shading indicates the distance from a given point on the surface to the mesh on the right as in Equation 1.

- The feature vector consists of the following properties,
- volume and extents of the overall head and neck region,
 - surface meshes of the mandible and outer body contour,
 - 3D centroid difference vector between mandible and hyoid,
 - 2D centroid difference vectors between hyoid and jugular veins, and between hyoid and spinal cord on the axial slice at the centroid of the hyoid,
 - normalized centroid locations of the hyoid and the mandible within the region.

5. EXPERIMENT AND RESULTS

All images are CT scans of head and neck cancer patients performed at the University of Washington Medical Center using a General Electric CT scanner. Thirty five sets of head and neck CT images were selected for the experiment in which all of the slices are 512×512 pixels in axial dimension; the distance between slices varies between 1.25 mm and 3.75 mm for each image set. A 3D deformable image registration process was run on a subset of images to generate lymph node region prediction, which was evaluated quantitatively using the Hausdorff distance. Figure 4 shows the correlation between the proposed distance measure and the result of 3D deformable image registration between selected patients. The Y-axis shows the Hausdorff distance between the transformed 3D mesh of the reference model lymph nodal region and the corresponding mesh of the test model using the transformation produced by the 3D deformable image registration. The X-axis represents the distance measurement, or the weighed Euclidian distance between the test and reference model properties in the feature vector space. Figure 4A compares this to results of lymph node region 1B of the right side, and 4B to lymph node region 2. The ideal result should demonstrate strict proportionality between x and y, where smaller distance between feature vectors indicates similar anatomy which should yield better alignment with image registration and smaller Hausdorff distance between the projected and expert drawn lymph node regions. While most data points in Figure 4 approximate x-y proportionality, few of them are not inline with the expectation. It is mainly due to inconsistent lymph node region contours drawn by various radiation oncologist experts that are affected by their clinical judgment, rather than purely following the image based classification. These results show promise for further investigation with a larger data set.

The experiment was performed on a Windows PC with Pentium 4 processor and 1GB of memory. The average time taken to calculate a distance measure between feature vectors of two models is approximately 3 seconds, including the ICP rigid body transformation and Hausdorff distance calculation between reference and target meshes. The mutual information based 3D deformable image registration process takes 20 minutes on average to register two sets of head and neck CT images. As we collect more data and increase the number of reference models, it becomes important to have a fast and effective method to select candidates of reference models that can produce the best result, such as the one proposed in this paper.

6. FUTURE WORK

We plan to extend and refine these methods into a software tool that utilizes domain knowledge and reference patients' information to generate potentially involved lymph node

region contours from target patient CT images. These contours can be used in existing radiation therapy systems as possible clinical target volumes for planning conformal radiation treatment.

We will investigate other potential features that can be incorporated in the similarity measure for better results, including more anatomical structures and their relationships. We will expand the test data set to refine and improve the similarity measure. It will be integrated into the tool to generate lymph node region contours. The performance of the tool will be clinically evaluated by radiation oncologists.

7. REFERENCES

- [1] P. Min, J.A. Halderman, M. Kazhdan, and T.A. Funkhouser, "Early experiences with a 3D model search engine", in *Web3D Symposium*, pp. 7-18, March 2003.
- [2] D.Y. Chen, X.P. Tian, Y.T. Shen, and M. Ouhyoung, "On visual similarity based 3D model retrieval", *Computer Graphics Forum (EG 2003 Proceedings)*, vol. 22, 2003.
- [3] J.W.H. Tangelder and R.C. Veltkamp, "Polyhedral model retrieval using weighted point sets", *International Journal of Image and Graphics*, vol. 3, pp. 209-229, 2003.
- [4] N. Iyer, S. Jayanti, K. Lou, Y. Kalyanaraman, and K. Ramani, "Three dimensional shape searching: State-of-the-art review and future trends", *Computer-Aided Design*, vol. 37, pp. 509-530.
- [5] J.W.H. Tangelder and R.C. Veltkamp, "A survey of content based 3D shape retrieval methods", *Proc. Shape Modeling International 2004 (SMI '04)*, vol. , pp. , 2005.
- [6] D. Mattes, D.R. Haynor, H. Vesselle, T.K. Lewellen, and W. Eubank, "PET-CT Image Registration in the Chest Using Free-form Deformations," *IEEE Trans. on Medical Imaging*, vol. 22, pp. 120-128, Jan. 2003.
- [7] C. Teng, L. G. Shapiro, and I. Kalet, "Head and neck lymph node region delineation using a hybrid image registration method", *Proc. IEEE International Symp. on Biomedical Imaging*, pp. 462-465, April 2006.
- [8] C. Teng, L. G. Shapiro, and I. Kalet, "Automatic segmentation of neck CT images", *Proc. 19th IEEE International Symp. on Computer-Based Medical Systems (CBMS)*, vol. , pp. , June 2006.
- [9] S. Ruiz-Correa, R.W. Sze, H.J. Lin, L.G. Shapiro, M.L. Speltz, and M.L. Cunningham, "Classifying craniosynostosis deformations by skull shape imaging", *Proc. 18th IEEE International Symp. on CBMS*, pp. 335-340, 2005.
- [10] N. Aspert, D. Santa-Cruz, and T. Ebrahimi, "MESH: Measuring errors between surfaces using the hausdorff distance", *Proc. of the IEEE International Conference in Multimedia and Expo (ICME) 2002*, vol. 1, pp. 705-70. August 2002.
- [11] P.J. Besl and N.D. McKay, "A method for registration of 3-d shapes", *IEEE Trans. PAMI*, vol. 14, pp. 239-256, Feb. 1992.
- [12] K.S.C. Chao, F.J. Wippold, G. Ozyigit, B.N. Tran, and J.F. Dempsey, "Determination and Delineation of Nodal Target volumes for Head-and-Neck Cancer Based on Patterns of Failure in Patients Receiving Definitive and Postoperative IMRT", *Int. J. of Radiation Oncology Biol. Phys.*, vol. 53, pp. 1174-1184, 2002.